

EXPLORING THE COSMOLOGICAL CONSEQUENCES OF JLA SUPERNOVA DATA WITH IMPROVED FLUX-AVERAGING TECHNIQUE

SHUANG WANG¹, SIXIANG WEN¹, MIAO LI¹

Draft version June 17, 2022

ABSTRACT

In this work, we explore the cosmological consequences of the “Joint Light-curve Analysis” (JLA) supernova (SN) data by using an improved flux-averaging (FA) technique, in which only the type Ia supernovae (SNe Ia) at high redshift are flux-averaged.

Adopting the criterion of figure of Merit (FoM) and considering four dark energy (DE) parameterizations, we search the best FA recipe that gives the tightest DE constraints in the $(z_{cut}, \Delta z)$ plane, where z_{cut} and Δz are redshift cut-off and redshift interval of FA, respectively. Then, based on the best FA recipe obtained, we discuss the impacts of varying z_{cut} and varying Δz , revisit the evolution of SN color luminosity parameter β , and study the effects of adopting different FA recipe on parameter estimation.

We find that: (1) The best FA recipe is $(z_{cut} = 0.6, \Delta z = 0.06)$, which is insensitive to a specific DE parameterization. (2) Flux-averaging JLA samples at $z_{cut} \geq 0.4$ will yield tighter DE constraints than the case without using FA. (3) Using FA can significantly reduce the redshift-evolution of β . (4) The best FA recipe favors a larger fractional matter density Ω_m . In summary, we present an alternative method of dealing with JLA data, which can reduce the systematic uncertainties of SNe Ia and give the tighter DE constraints at the same time. Our method will be useful in the use of SNe Ia data for precision cosmology.

Subject headings: Cosmology: dark energy, observations, cosmological parameters

1. INTRODUCTION

Type Ia supernovae (SNe Ia) are a sub-category of cataclysmic variable stars that results from the violent explosion of a white dwarf star in a binary system (Hillebrandt et al. 2000). SNe Ia can be used as standard candle to measure the cosmic distance (Riess et al. 1998; Perlmutter et al. 1999; Astier et al. 2006), and thus have become one of the most powerful tools to probe the nature of dark energy (DE) (Frieman et al. 2008; Li et al. 2011a, 2013a; Weinberg et al. 2013). In the recent decade, several high quality supernova (SN) data-sets were released, such as “Union” (Kowalski et al. 2008), “Constitution” (Hicken et al. 2009a,b), “SDSS” (Kessler et al. 2009), “Union2” (Amanullah et al. 2010), “SNLS3” (Conley et al. 2011) and “Union2.1” (Suzuki et al. 2012). In a latest paper, the “Joint Light-curve Analysis” (JLA) data (Betoule et al. 2014), which consisting of 740 SNe Ia, was released. This SN sample has been widely studied in the literature.

As the rapid growth of the number of SNe discovered in the astronomical observation, the control of the systematic uncertainties of SNe Ia have drawn more and more attention in recent years. For examples, the studies on various SNe Ia data-sets, such as SNLS3 (Wang & Wang 2013a), Union2.1 (Mohlberg & Ralston 2013), Pan-STARRS1 (Scolnic et al. 2014) and JLA (Shariff et al. 2015; Li et al. 2016), all indicated that SN color luminosity parameter β should evolve along with redshift z at high confidence level (CL); it has also been proved that the evolution of β has significant effects on the parameter estimation of various cosmological models (Wang et al. 2014a,b,c, 2015). Besides, it was found that the intrinsic scatter σ_{int} has the hint of redshift-dependence that

will affect the results of cosmology fits (Marriner 2011). In addition, another factor that causes SN systematic uncertainties is the choice of light-curve fitters (LCF) (Kessler et al. 2009): for instance, adopting “MLCS2k2” (Jha et al. 2007) and “SALT2” (Guy et al. 2007) LCF will lead to completely different fitting results (Pigozzo et al. 2011; Bengochea et al. 2014); in contrast, using “SALT2” and “SiFTO” (Conley et al. 2011) LCF will yield the consistent fitting results (Wang et al. 2016).

Instead of analysing the factors of SN systematic uncertainties one by one, an alternative is to deal with these factors in an unified framework. In 2000, Wang proposed a data analysis technique, called flux-averaging (FA) (Wang 2000), to reduce the systematic uncertainties caused by the weak lensing of SNe Ia. The key idea is that due to flux conservation in gravitational lensing, the average flux of a large number of SNe Ia at the same redshift should be unity; thus averaging the observed flux from a large number of SNe Ia at the same redshift can recover the unlensed brightness of the SNe Ia at that redshift (Wang & Mukherjee 2004). In a series of research works, Wang and the collaborators have applied the FA technique to give the cosmological constraints on DE (Wang & Tegmark 2004; Wang & Mukherjee 2006, 2007; Wang 2008), and have found that using FA can also reduce the bias in distance estimate induced by some other systematic effects (Wang & Tegmark 2005; Wang 2009; Wang et al. 2012).

The original FA method is to average the observed flux of all the SN samples. For this case, FA only relates to one quantity: the redshift interval Δz . In (Wang & Wang 2013a), one of the present author and Wang proposed an improved version of FA, in which only the SN data at high-redshift are flux-averaged. For this new FA method, another quantity, redshift cut-off z_{cut} , is introduced. For the SN samples at $z < z_{cut}$, the χ^2 is computed by using the usual “magnitude statistics”; for the SN samples at $z \geq z_{cut}$, the χ^2 is computed by using the “flux statistics”. In a recent work, Wang and Dai applied

wangshuang@mail.sysu.edu.cn (Corresponding author)
wensx@mail2.sysu.edu.cn
limiao9@mail.sysu.edu.cn

¹ School of Physics and Astronomy, Sun Yat-Sen University, Guangzhou 510275, P. R. China

this improved FA technique to explore the JLA SN sample, and found that it can give tighter constraints on DE (Wang & Dai 2015). However, some important factors are not taken into account in (Wang & Dai 2015). For example, only one kind of FA recipe, $(z_{cut} = 0.5, \Delta z = 0.04)$, is used in (Wang & Dai 2015). This choice of $(z_{cut}, \Delta z)$ may not be the best FA recipe that can give the tightest DE constraints. In addition, only one kind of DE parameterization, i.e. the Chevallier-Polarski-Linder (CPL) model (Chevallier & Polarski 2001; Linder 2003), is used in (Wang & Dai 2015). So the conclusions of (Wang & Dai 2015) may depend on the specific model. Moreover, only the fitting results of the CPL model are briefly discussed in (Wang & Dai 2015), while the impacts of adopting FA on the systematic uncertainties of JLA sample are not discussed.

The aim of our work is to present a systematic and comprehensive investigation on the cosmological consequences of the JLA data-set by using the improved FA method. Compared with previous literature, the novelty of our work are as follows: (1) Quite different from the previous studies, we scan the whole $(z_{cut}, \Delta z)$ plane to search the best FA recipe, by adopting the criterion of the dark energy task force (DETF) figure of Merit (FoM) (Albrecht et al. 2006). (2) To ensure that our results are insensitive to a specific DE model, four kinds of DE parameterizations, including the CPL model, the Jassal-Bagla-Padmanabhan (JBP) model (Jassal et al. 2005a,b), the Barbosa-Alcaniz (BA) model (Barboza & Alcaniz 2008) and the Wang (WANG) model (Wang 2008) are taken into account. (3) Based on the best FA recipe obtained in this work, we discuss the impacts of varying z_{cut} and varying Δz , revisit the evolution of SN color luminosity parameter β , and study the effects of adopting different FA recipe on parameter estimation.

In addition to the JLA SN data, we also use the galaxy clustering (GC) measurements of Hubble parameter $H(z)$ and angular diameter distance $D_A(z)$ (Wang & Dai 2015) extracted from the Sloan Digital Sky Survey (SDSS) at $z = 0.35$ (SDSS DR7 (Chuang & Wang 2012)) and $z = 0.57$ (BOSS DR11 (Anderson et al. 2014)), as well as the cosmic microwave background (CMB) distance priors $(l_a, R, \Omega_b h^2)$ derived from the 2015 Planck data (Ade et al. 2015).

We describe our method in Section 2, present our results in Section 3, and summarize in Section 4.

2. METHODOLOGY

In this section, we briefly introduce the four DE parameterization models, and then describe the observational data used in the present work.

2.1. Theoretical Model

In a flat universe,² the comoving distance $r(z)$ to an object is given by

$$r(z) = cH_0^{-1} \int_0^z \frac{dz'}{E(z')}, \quad (1)$$

where c is the speed of light, and H_0 is the Hubble constant. $E(z)$ is the reduced Hubble parameter, which satisfies

$$E(z) = \sqrt{\Omega_r(1+z)^4 + \Omega_m(1+z)^3 + \Omega_{de}X(z)}, \quad (2)$$

² The assumption of flatness is motivated by the inflation scenario. For a detailed discussion of the effects of spatial curvature, see (Clarkson, Cortes, & Bassett 2007)

where Ω_r , Ω_m and Ω_{de} are the present fractional densities of radiation, matter and DE, respectively. Per Ref. (Wang & Wang 2013b), we take $\Omega_r = \Omega_m/(1+z_{eq})$, where $z_{eq} = 2.5 \times 10^4 \Omega_m h^2 (T_{cmb}/2.7 \text{ K})^{-4}$, $T_{cmb} = 2.7255 \text{ K}$, and h is the Hubble constant. Note that $\Omega_r + \Omega_m + \Omega_{de} = 1$, so Ω_{de} is not a model parameter. In addition, $X(z)$ is the DE density function, which satisfies

$$X(z) = \exp \left[3 \int_0^z dz' \frac{1+w(z')}{1+z'} \right]. \quad (3)$$

Here w is the equation of state (EoS) of DE, which is the key element to determine the properties of DE. For the simplest Λ -cold-dark-matter (Λ CDM) model, $X = 1$.

To study the impacts of different $w(z)$, here we consider four popular parametrization models:

- The CPL model. It has a dynamical EoS $w(z) = w_0 + w_a \frac{z}{1+z}$, then

$$X(z) = (1+z)^{3(1+w_0+w_a)} e^{\frac{-3w_a z}{1+z}}. \quad (4)$$

- The JBP model (Jassal et al. 2005a,b). It has a dynamical EoS $w(z) = w_0 + w_a \frac{z}{(1+z)^2}$, then

$$X(z) = (1+z)^{3(1+w_0)} e^{\frac{3w_a z^2}{2(1+z)^2}}. \quad (5)$$

- The BA model (Barboza & Alcaniz 2008). It has a dynamical EoS $w(z) = w_0 + w_a \frac{z(1+z)}{1+z^2}$, then

$$X(z) = (1+z)^{3(1+w_0)} (1+z^2)^{\frac{3w_a}{2}}. \quad (6)$$

- The WANG model (Wang 2008). It has a dynamical EoS $w(z) = w_0 \frac{1-2z}{1+z} + w_a \frac{z}{(1+z)^2}$, then

$$X(z) = (1+z)^{3(1-2w_0+3w_a)} e^{\frac{9(w_0-w_a)z}{1+z}}. \quad (7)$$

For each model, the parameter w_0 represent the current value of EoS, and the parameter w_a reflect the evolution of EoS.

In 2006, the DETF team proposed a quantity, called FoM, to quantitatively assess the ability of constraining DE of an experiment project. FoM is defined as the reciprocal of the error ellipse area enclosing the 95% confidence limit in the $w_0 - w_a$ plane of the CPL model. It satisfies

$$FoM = \frac{1}{6.17\pi [\det Cov(w_0, w_a)]^{1/2}}, \quad (8)$$

where $Cov(w_0, w_a)$ is covariance matrix of w_0 and w_a . It is clear that a larger FoM indicates a better accuracy. In this work, we extend the application scope of FoM to the cases of other DE parametrization. Moreover, as mentioned above, based on the criterion of FoM, we will search the best FA recipe that can give the tightest DE constraints.

2.2. Observational Data

In this section, firstly, we introduce how to calculate the χ^2 of JLA data using the usual ‘‘magnitude statistics’’. Then, we introduce how to calculate the χ^2 of JLA data using the ‘‘flux statistics’’, as well as the details of the improved FA method. At last, we briefly introduce other observational data used in this work.

Theoretically, the distance modulus μ_{th} in a flat universe can be written as

$$\mu_{th} = 5 \log_{10} \left[\frac{d_L(z_{hel}, z_{cmb})}{Mpc} \right] + 25, \quad (9)$$

where z_{cmb} and z_{hel} are the CMB restframe and heliocentric redshifts of SN. The luminosity distance d_L is given by

$$d_L(z_{hel}, z_{cmb}) = (1 + z_{hel})r(z_{cmb}), \quad (10)$$

where $r(z)$ has been given in Eq. 1.

The observation of distance modulus μ_{obs} is given by a empirical linear relation:

$$\mu_{obs} = m_B^* - M_B + \alpha \times X_1 - \beta \times C, \quad (11)$$

where m_B^* is the observed peak magnitude in the rest-frame of the B band, X_1 describes the time stretching of light-curve, C describes the supernova color at maximum brightness and M_B is the absolute B-band magnitude, which depends on the host galaxy properties (Schlafly & Finkbeiner 2011; Johansson et al. 2013). Notice that M_B is related to the host stellar mass $M_{stellar}$ by a simple step function (Betoule et al. 2014)

$$M_B = \begin{cases} M_B^1 & \text{if } M_{stellar} < 10^{10} M_\odot, \\ M_B^2 & \text{otherwise.} \end{cases} \quad (12)$$

Here M_\odot is the mass of sun.

The χ^2 of JLA data can be calculated as

$$\chi_{SN}^2 = \Delta\mu^T \cdot \mathbf{Cov}^{-1} \cdot \Delta\mu, \quad (13)$$

where $\Delta\mu \equiv \mu_{obs} - \mu_{th}$ is the data vector and \mathbf{Cov} is the total covariance matrix, which is given by

$$\mathbf{Cov} = \mathbf{D}_{stat} + \mathbf{C}_{stat} + \mathbf{C}_{sys}. \quad (14)$$

Here \mathbf{D}_{stat} is the diagonal part of the statistical uncertainty, which is given by (Betoule et al. 2014),

$$\begin{aligned} \mathbf{D}_{stat,ii} = & \left[\frac{5}{z_i \ln 10} \right]^2 \sigma_{z,i}^2 + \sigma_{int}^2 + \sigma_{lensing}^2 + \sigma_{m_B,i}^2 \\ & + \alpha^2 \sigma_{X_1,i}^2 + \beta^2 \sigma_{C,i}^2 + 2\alpha C_{m_B X_1,i} - 2\beta C_{m_B C,i} \\ & - 2\alpha\beta C_{X_1 C,i}, \end{aligned} \quad (15)$$

where the first three terms account for the uncertainty in redshift due to peculiar velocities, the intrinsic variation in SN magnitude and the variation of magnitudes caused by gravitational lensing. $\sigma_{m_B,i}^2$, $\sigma_{X_1,i}^2$, and $\sigma_{C,i}^2$ denote the uncertainties of m_B , X_1 and C for the i -th SN. In addition, $C_{m_B X_1,i}$, $C_{m_B C,i}$ and $C_{X_1 C,i}$ are the covariances between m_B , X_1 and C for the i -th SN. Moreover, \mathbf{C}_{stat} and \mathbf{C}_{sys} are the statistical and the systematic covariance matrices, given by

$$\mathbf{C}_{stat} + \mathbf{C}_{sys} = V_0 + \alpha^2 V_a + \beta^2 V_b + 2\alpha V_{0a} - 2\beta V_{0b} - 2\alpha\beta V_{ab}, \quad (16)$$

where V_0 , V_a , V_b , V_{0a} , V_{0b} and V_{ab} are matrices given by the JLA group.

As pointed out in (Betoule et al. 2014), in the process of calculating χ_{SN}^2 , the absolute B-band magnitude M_B is marginalized. So in this work, we follow the procedure of (Betoule et al. 2014), and do not treat M_B as free parameter. We refer the reader to Ref. (Betoule et al. 2014) for the details of calculating χ_{SN}^2 .

Now, let us turn to the FA of JLA data. FA is a very useful technique to reduce the bias in distance estimate induced by various systematic effects (Wang & Mukherjee 2004; Wang & Tegmark 2005; Wang 2009). The original FA method divide the whole redshift region of SNe Ia into a lot of bins, where the redshift interval of each bin is Δz . Then, for the JLA SN data in each bin, the steps of FA are as follows (Wang et al. 2012):

(1) Convert the distance modulus of SNe Ia into “fluxes”,

$$F(z_l) \equiv 10^{-(\mu_0^{data}(z_l) - 25)/2.5} = \left(\frac{d_L^{data}(z_l)}{\text{Mpc}} \right)^{-2}. \quad (17)$$

Here z_l represent the CMB restframe redshift of SN.

(2) For a given set of cosmological parameters $\{s\}$, obtain “absolute luminosities”, $\{\mathcal{L}(z_l)\}$, by removing the redshift dependence of the “fluxes”, i.e.,

$$\mathcal{L}(z_l) \equiv d_L^2(z_l|s) F(z_l). \quad (18)$$

(3) Flux-average the “absolute luminosities” $\{\mathcal{L}_l^i\}$ in each redshift bin i to obtain $\{\bar{\mathcal{L}}^i\}$:

$$\bar{\mathcal{L}}^i = \frac{1}{N_i} \sum_{l=1}^{N_i} \mathcal{L}_l^i(z_l^{(i)}), \quad \bar{z}_i = \frac{1}{N_i} \sum_{l=1}^{N_i} z_l^{(i)}. \quad (19)$$

(4) Place $\bar{\mathcal{L}}^i$ at the mean redshift \bar{z}_i of the i -th redshift bin, now the binned flux is

$$\bar{F}(\bar{z}_i) = \bar{\mathcal{L}}^i / d_L^2(\bar{z}_i|s). \quad (20)$$

with the corresponding flux-averaged distance modulus:

$$\bar{\mu}^{data}(\bar{z}_i) = -2.5 \log_{10} \bar{F}(\bar{z}_i) + 25. \quad (21)$$

(5) Compute the covariance matrix of $\bar{\mu}(\bar{z}_i)$ and $\bar{\mu}(\bar{z}_j)$:

$$\begin{aligned} \text{Cov} [\bar{\mu}(\bar{z}_i), \bar{\mu}(\bar{z}_j)] &= \frac{1}{N_i N_j \bar{\mathcal{L}}^i \bar{\mathcal{L}}^j} \cdot \\ & \sum_{l=1}^{N_i} \sum_{m=1}^{N_j} \mathcal{L}(z_l^{(i)}) \mathcal{L}(z_m^{(j)}) \langle \Delta\mu_0^{data}(z_l^{(i)}) \Delta\mu_0^{data}(z_m^{(j)}) \rangle \end{aligned} \quad (22)$$

where $\langle \Delta\mu_0^{data}(z_l^{(i)}) \Delta\mu_0^{data}(z_m^{(j)}) \rangle$ is the covariance of the measured distance moduli of the l -th SN Ia in the i -th redshift bin, and the m -th SN Ia in the j -th redshift bin. $\mathcal{L}(z)$ is defined by Eqs.(17) and (18).

(6) For the flux-averaged data, $\{\bar{\mu}(\bar{z}_i)\}$, compute

$$\chi_{SN}^2 = \sum_{ij} \Delta\bar{\mu}(\bar{z}_i) \text{Cov}^{-1} [\bar{\mu}(\bar{z}_i), \bar{\mu}(\bar{z}_j)] \Delta\bar{\mu}(\bar{z}_j) \quad (23)$$

where

$$\Delta\bar{\mu}(\bar{z}_i) \equiv \bar{\mu}(\bar{z}_i) - \mu^P(\bar{z}_i|s), \quad (24)$$

and

$$\mu^P(\bar{z}_i) = -2.5 \log_{10} F^P(\bar{z}_i) + 25. \quad (25)$$

with $F^P(\bar{z}_i|s) = (d_L(z|s)/\text{Mpc})^{-2}$.

As mentioned above, the improved FA method (Wang & Wang 2013a) introduce a new quantity: the redshift cut-off z_{cut} . For the SN samples at $z < z_{cut}$, the χ^2 is computed by using the usual “magnitude statistics” (i.e., Eq. 13); for the SN samples at $z \geq z_{cut}$, the χ^2 is computed by using the “flux statistics” (i.e., Eq. 23). In (Wang & Dai 2015), Wang and Dai applied this improved FA method to explore the JLA data-set, and found that it can give tighter constraints on DE. However, only one kind of FA recipe, ($z_{cut} = 0.5$, $\Delta z = 0.04$), is considered in (Wang & Dai 2015). This choice of z_{cut} and Δz may not be the best FA recipe that can give the tightest DE constraints. In order to find out the best FA recipe, by adopting

the criterion of DETF FoM , we scan the whole $(z_{cut}, \Delta z)$ plane in this work. Specifically, we set that $z_{cut} = 0.1i$, $i = 0, 1, 2, \dots, 8$ and $\Delta z = 0.01j$, $j = 1, 2, 3, \dots, 10$.

In addition to the JLA SN data, we also use the GC and the CMB data to improve the constraint results of DE. For the GC data, we use the measurements of $H(z)$ and $D_A(z)$ (Wang & Dai 2015) extracted from the SDSS DR7 at $z = 0.35$ and the BOSS DR11 at $z = 0.57$. For the CMB data, we use the distance priors $(l_a, R, \Omega_b h^2)$ derived from the 2015 Planck data (Ade et al. 2015).³ For simplicity, here we do not describe how to include the GC and the CMB data into the χ^2 statistics. For the details of calculating the χ^2 function of the GC data, see Ref. (Wang & Dai 2015); for the details of computing the χ^2 function of the CMB data, see Ref. (Ade et al. 2015).

We perform a MCMC likelihood analysis (Lewis & Bridle 2002) to obtain $O(10^6)$ samples for each set of results presented in this paper. In this work we choose $(\alpha, \beta, \Omega_m, \Omega_b h^2, h, w_0, w_a)$ as a set of free parameters. We assume flat priors for all the parameters, and allow ranges of the parameters wide enough such that further increasing the allowed ranges has no impact on the results.

3. RESULTS

This section include four parts. Firstly, by scanning the whole $(z_{cut}, \Delta z)$ plane, we find out the best FA recipe that can yield the largest value of DETF FoM . Secondly, based on the CPL model and the best FA recipe, we discuss the impacts of varying z_{cut} and varying Δz . Thirdly, by combining FA with redshift tomography technique, we revisit the evolution of β for the JLA data. fourthly, by using the JLA data alone, we study the impacts of adopting different FA recipe on parameter estimation.

3.1. Searching The Best FA Recipe

To search the best FA recipe, we scan the whole $(z_{cut}, \Delta z)$ plane. For each choice of $(z_{cut}, \Delta z)$, we perform a MCMC analysis for the CPL model, and then calculate the corresponding value of FoM . In Fig. 1, we plot a 3D graph, which show the results of FoM given by different choices of $(z_{cut}, \Delta z)$. It should be mentioned that the combined SN+GC+CMB data are used in the analysis. From this figure we can see that, the original FA method (i.e., $z_{cut} = 0$) always give a small FoM ; in contrast, the improved FA recipe with a $(z_{cut}$ at high redshift will yield a larger FoM . This means that the improved FA recipe can give better DE constraints than the original FA recipe. Moreover, we find out the best FA recipe ($z_{cut} = 0.6, \Delta z = 0.06$) (the blue star), which can give a largest $FoM = 4.6965$. As a comparison, in (Wang & Dai 2015), Wang and Dai adopted the FA recipe ($z_{cut} = 0.5, \Delta z = 0.04$) (the blue round dot), which give a $FoM = 4.6083$. therefore, we can conclude that our FA recipe can give tighter DE constraints than the recipe of (Wang & Dai 2015). This shows the importance of finding out the best FA recipe.

Let us discuss this topic with more details. Table 1 show the cosmology-fits results for the CPL, the JBP, the BA and the WANG models, given by different FA recipe. Both the best-fit result and the 1σ errors of various parameters, as well as the corresponding results of FoM , are listed in this table. “No FA” denote the case without using FA, “Original FA” represent

the FA recipe ($z_{cut} = 0, \Delta z = 0.06$), “Best FA” correspond to the FA recipe ($z_{cut} = 0.6, \Delta z = 0.06$). From this table we can see that, for all the four DE models, adopting the “Best FA” recipe will yield a larger β and a larger Ω_m , compared with the cases of “No FA” and “Original FA”. Moreover, among these three FA recipes, the “Original FA” recipe always give the smallest FoM , while the “Best FA” recipe always give the largest FoM . This means that the “Best FA” recipe can yield tightest DE constraints. Since this result holds true for all the four DE parameterizations, our conclusion is insensitive to the specific DE model considered in the background.

3.2. The Impacts of Varying z_{cut} And Varying Δz

Based on the CPL model and the best FA recipe, we further investigate the effects of varying z_{cut} and varying Δz . In Fig. 2, we give results of FoM given by different z_{cut} (left panel) and different Δz (right panel). Note that the combined SN+GC+CMB data are used in the analysis. To make a comparison, we also give the result of FoM (dashed line) for the case without using FA. From the left panel of Fig. 2, we find that varying z_{cut} will significantly affect the result of FoM : if $z_{cut} < 0.4$, then using FA will yield a smaller FoM than the result of “NO FA” case; if $z_{cut} \geq 0.4$, then using FA will yield a larger FoM than the result of “NO FA” case. In other words, flux-averaging JLA samples at $z_{cut} \geq 0.4$ will yield tighter DE constraints than the case without using FA. In (Wang & Dai 2015), Wang and Dai argued that flux-averaging JLA samples at $z_{cut} \geq 0.5$ will yield tighter constraints. Since only one kind of FA recipe ($z_{cut} = 0.5, \Delta z = 0.04$) was considered in (Wang & Dai 2015), it is clear that our conclusion is more accurate. In addition, from the left panel of Fig. 2 we find that, once $z_{cut} = 0.6$ is fixed, adopting FA will always yield a larger FoM than the result of “NO FA” case. This means that, compared with the case of varying z_{cut} , the effects of varying Δz are much smaller.

3.3. The Revisit of The Redshift-Evolution of β

In a previous paper (Li et al. 2016), we studied the evolution of β for the JLA data by using the redshift tomography (RT) technique. The basic idea of RT is to divide the SN data into different redshift bins, assuming that β is a piecewise constant. Then one can constrain Λ CDM model and check the consistency of cosmology-fit results in each bin. It was found that, for the JLA data-set, β has a significant trend of decreasing at high redshift. It must be stressed that only the usual “magnitude statistics” was used in (Li et al. 2016), while the FA of SNe Ia was not taken into account. It will be interesting to study the effects of adopting FA technique on β ’s evolution.

We revisit the evolution of β for the JLA sample by combining FA with RT technique. For the RT, we divide the SN data into two redshift bins with a discontinuity point $z_{cut} = 0.6$; for the FA, we adopt the FA recipe ($z_{cut} = 0.6, \Delta z = 0.01$), which has more data points at high redshift than the best FA recipe. In Fig. 3, we plot the best-fit results (left panel) and the 1σ regions (right panel) of β given by different SN analysis technique. “No FA (No RT)” denotes the case without using FA and redshift tomography. “No FA (With RT)” represents the case only using redshift tomography with $z_{cut} = 0.6$. “FA (With RT)” corresponds to the case using best FA and redshift tomography with $z_{cut} = 0.6$. Here we study the Λ CDM model; besides, only the JLA SN data are used in the analysis. Note that the results of β at low redshift give by “No FA (With RT)” and “FA (With RT)” are the same, because the improve

³ In addition to (Ade et al. 2015), there are some other CMB distance priors data, e.g. see Refs. (Wang & Wang 2013b; Huang et al. 2015; Wang & Dai 2015).

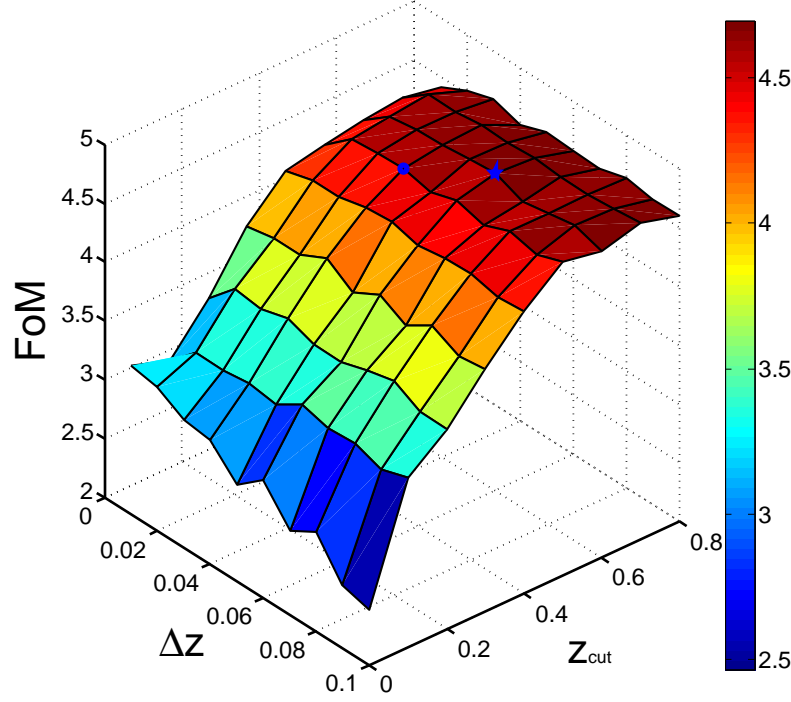


FIG. 1.— The 3D graph that show the results of FoM given by different choices of $(z_{cut}, \Delta z)$, for the CPL model. Here the combined SN+GC+CMB data are used in the analysis. Note that $z_{cut} = 0.1i$, $i = 0, 1, 2, \dots, 8$; while $\Delta z = 0.01j$, $j = 1, 2, 3, \dots, 10$. The blue star denotes the best FA recipe ($z_{cut} = 0.6, \Delta z = 0.06$), which can give a largest $FoM = 4.6965$. The blue round dot represents the recipe of (Wang & Dai 2015) ($z_{cut} = 0.5, \Delta z = 0.04$), which give a $FoM = 4.6083$.

TABLE 1

COSMOLOGY-FITS RESULTS FOR THE CPL, THE JBP, THE BA AND THE WANG MODELS, GIVEN BY DIFFERENT FA RECIPE. BOTH THE BEST-FIT RESULT AND THE 1σ ERRORS OF VARIOUS PARAMETERS, AS WELL AS THE CORRESPONDING RESULTS OF FoM , ARE LISTED IN THIS TABLE. “NO FA” DENOTE THE CASE WITHOUT USING FA, “ORIGINAL FA” REPRESENT THE FA RECIPE ($z_{cut} = 0, \Delta z = 0.06$), “BEST FA” CORRESPOND TO THE FA RECIPE ($z_{cut} = 0.6, \Delta z = 0.06$). THE COMBINED SN+GC+CMB DATA ARE USED IN THE ANALYSIS.

Parm	CPL			JBP			BA			Wang		
	No FA	Original FA	Best FA	No FA	Original FA	Best FA	No FA	Original FA	Best FA	No FA	Original FA	Best FA
α	$0.140^{+0.013}_{-0.012}$	$0.0798^{+0.112}_{-0.093}$	$0.140^{+0.016}_{-0.016}$	$0.141^{+0.012}_{-0.013}$	$0.0898^{+0.099}_{-0.104}$	$0.140^{+0.017}_{-0.016}$	$0.141^{+0.012}_{-0.013}$	$0.0818^{+0.110}_{-0.097}$	$0.139^{+0.017}_{-0.015}$	$0.140^{+0.013}_{-0.012}$	$0.0754^{+0.115}_{-0.089}$	$0.139^{+0.017}_{-0.015}$
β	$3.109^{+0.152}_{-0.163}$	$3.088^{+0.908}_{-0.730}$	$3.258^{+0.194}_{-0.206}$	$3.096^{+0.165}_{-0.150}$	$3.019^{+1.014}_{-0.662}$	$3.252^{+0.206}_{-0.198}$	$3.098^{+0.167}_{-0.156}$	$3.067^{+0.919}_{-0.694}$	$3.220^{+0.233}_{-0.171}$	$3.094^{+0.166}_{-0.150}$	$3.117^{+0.892}_{-0.731}$	$3.232^{+0.216}_{-0.182}$
h	$0.684^{+0.024}_{-0.024}$	$0.683^{+0.041}_{-0.032}$	$0.675^{+0.028}_{-0.030}$	$0.683^{+0.025}_{-0.023}$	$0.687^{+0.025}_{-0.036}$	$0.679^{+0.026}_{-0.032}$	$0.681^{+0.022}_{-0.022}$	$0.685^{+0.038}_{-0.034}$	$0.670^{+0.025}_{-0.025}$	$0.682^{+0.026}_{-0.022}$	$0.686^{+0.037}_{-0.035}$	$0.671^{+0.033}_{-0.027}$
Ω_m	$0.299^{+0.023}_{-0.020}$	$0.298^{+0.031}_{-0.033}$	$0.305^{+0.031}_{-0.024}$	$0.299^{+0.023}_{-0.020}$	$0.297^{+0.033}_{-0.033}$	$0.301^{+0.031}_{-0.024}$	$0.301^{+0.021}_{-0.022}$	$0.298^{+0.033}_{-0.031}$	$0.310^{+0.027}_{-0.029}$	$0.301^{+0.020}_{-0.022}$	$0.296^{+0.034}_{-0.030}$	$0.309^{+0.026}_{-0.029}$
$\Omega_b h^2$	$0.0226^{+0.0005}_{-0.0005}$	$0.0226^{+0.0005}_{-0.0005}$	$0.0227^{+0.0005}_{-0.0006}$	$0.0226^{+0.0005}_{-0.0005}$	$0.0225^{+0.0006}_{-0.0006}$	$0.0226^{+0.0006}_{-0.0006}$	$0.0226^{+0.0005}_{-0.0005}$	$0.0225^{+0.0006}_{-0.0006}$	$0.0226^{+0.0006}_{-0.0006}$	$0.0225^{+0.0005}_{-0.0005}$	$0.0226^{+0.0006}_{-0.0006}$	$0.0226^{+0.0006}_{-0.0005}$
w_0	$-0.996^{+0.228}_{-0.184}$	$-1.002^{+0.320}_{-0.318}$	$-0.976^{+0.280}_{-0.228}$	$-0.996^{+0.326}_{-0.307}$	$-1.052^{+0.507}_{-0.474}$	$-1.070^{+0.365}_{-0.383}$	$-0.984^{+0.193}_{-0.176}$	$-0.993^{+0.284}_{-0.284}$	$-0.9426^{+0.219}_{-0.230}$	$-0.974^{+0.213}_{-0.210}$	$-1.010^{+0.321}_{-0.321}$	$-0.940^{+0.228}_{-0.261}$
w_a	$0.026^{+0.633}_{-1.024}$	$0.078^{+0.830}_{-1.274}$	$0.119^{+0.647}_{-0.988}$	$0.094^{+1.835}_{-2.273}$	$0.323^{+2.606}_{-2.96}$	$0.684^{+2.219}_{-2.090}$	$0.011^{+0.330}_{-0.512}$	$-0.006^{+0.464}_{-0.557}$	$0.028^{+0.358}_{-0.460}$	$-0.986^{+0.109}_{-0.167}$	$-0.986^{+0.128}_{-0.193}$	$-0.938^{+0.113}_{-0.151}$
FoM	4.3204	3.0013	4.6965	1.8292	1.1796	1.8429	8.8308	6.0789	9.0573	13.1388	8.9052	14.0444

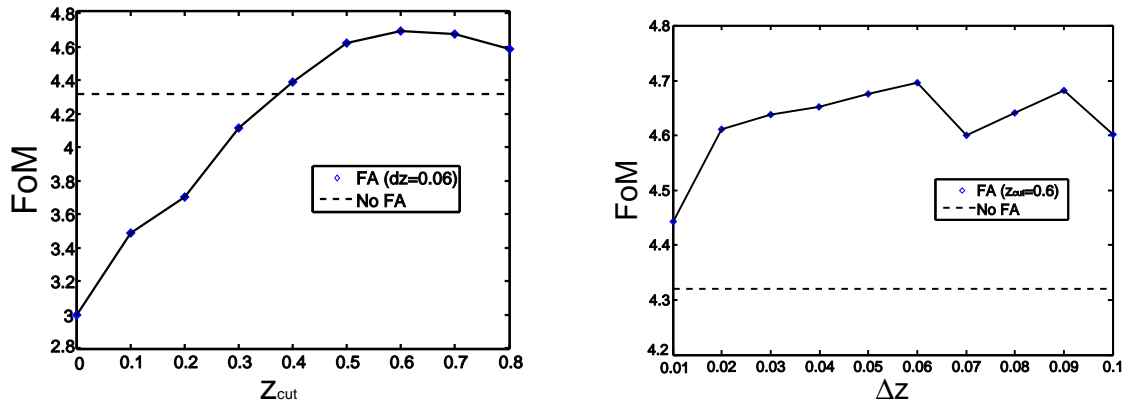


FIG. 2.— The results of FoM given by different z_{cut} (left panel) and different Δz (right panel), for the CPL model. Here the combined SN+GC+CMB data are used in the analysis. For the left panel, $\Delta z = 0.06$ is always fixed; for the right panel, $z_{cut} = 0.6$ is always fixed. For comparison, we also give the result of FoM (dashed line) for the case without using FA.

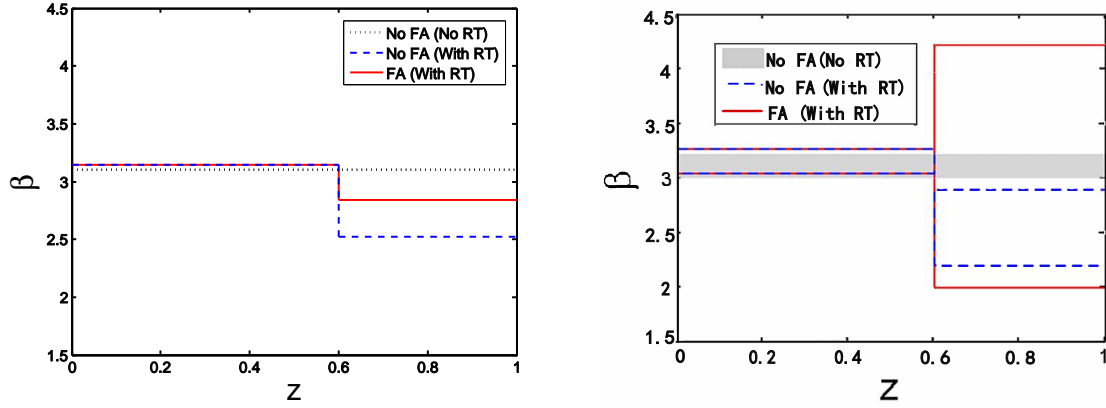


FIG. 3.— The best-fit results (left panel) and the 1σ regions (right panel) of β at redshift region $[0, 1]$ given by different SN analysis technique. “No FA (No RT)” denotes the case without using FA and redshift tomography. “No FA (With RT)” represents the case only using redshift tomography with $z_{cut} = 0.6$. “FA (With RT)” corresponds to the case using best FA and redshift tomography with $z_{cut} = 0.6$. For the left panel, the black dotted line, the blue dashed line and the red solid line correspond to the best-fit results of β of “No FA (No RT)”, “No FA (With RT)” and “FA (With RT)”, respectively. For the right panel, the grey region, the region inside blue dashed lines and the region inside red solid lines correspond to the 1σ regions of β of “No FA (No RT)”, “No FA (With RT)” and “FA (With RT)”, respectively. Note that we adopt the Λ CDM model; besides, only the JLA SN data are used in the analysis.

FA technique only flux-average SNe Ia at high redshift. From the left panel of Fig. 3 we find that, only using RT will yield a significant decrease for the best-fit result of β at $z_{cut} \geq 0.6$, which is consistent with result of (Li et al. 2016). In contrast, adopting FA will yield a larger best-fit value of β at $z_{cut} \geq 0.6$, which is much closer to the result of the “No FA (No RT)” case. From the right panel of Fig. 3 we see that, if only using RT, the 1σ region of β at $z_{cut} \geq 0.6$ will significantly deviate from the 1σ region at $z_{cut} < 0.6$, as well as the “No FA (With RT)” case. In contrast, after adopting FA, the 1σ region of β at $z_{cut} \geq 0.6$ will be consistent with the 1σ region at $z_{cut} < 0.6$, as well as the “No FA (With RT)” case. These results show that using FA can significantly reduce the redshift-evolution of β .

3.4. The Impacts of Adopting Different FA Recipe on Parameter Estimation

At last, let us discuss the impacts of adopting different FA recipe on parameter estimation. For simplicity, here we just consider the standard cosmological model: the Λ CDM model. In addition, in this subsection, we make use of the JLA SN data alone to perform the MCMC analysis.

In Fig. 4, we plot the 1D marginalized probability distributions of Ω_m given by different FA recipe, for the Λ CDM model. Note that “No FA” (black dotted line) denotes the case without using FA, “Original FA” (blue dashed line) represents the FA recipe ($z_{cut} = 0, \Delta z = 0.06$), “Best FA” (red solid line) corresponds to the FA recipe ($z_{cut} = 0.6, \Delta z = 0.06$). It can be seen that, the original FA recipe will give a smaller Ω_m , while the best FA recipe will give a larger Ω_m . The best-fit values of Ω_m given by “No FA”, “Original FA” and “Best FA” are 0.2929, 0.2829 and 0.3478, respectively. It is very interesting to note that the enlarge of Ω_m had also been found in (Li et al. 2016), in which the impacts of β ’s evolution on parameter estimation are taken into account. In other word, both adopting the best FA method and considering the evolution of β will yield a larger Ω_m . As a comparison, we also plot the corresponding result given by the FA recipe (green dashed-dotted line). For this case, the best-fit value of Ω_m is 0.2982, which is closer to the case of “No FA”. However, all the results of Ω_m given by these three FA recipes are still consistent with the result given by the FA recipe, at 1σ confidence level.

In Fig. 5, we plot the 1σ regions of reduced Hubble parameter $E(z)$ (left panel) and deceleration parameter $q(z)$ (right panel) at redshift region $[0, 1]$ given by different FA recipe, for the Λ CDM model. The left panel of Fig. 5 shows that adopting the original FA recipe will yield a smaller $E(z)$ at high redshift, while adopting the best FA recipe will yield a larger $E(z)$ at high redshift. The right panel of Fig. 5 shows that making use of the original FA recipe will yield a smaller $q(z)$, while adopting the best FA recipe will yield a larger $q(z)$. In other words, the best FA recipe favors a universe with a smaller acceleration. This result is consistent with the result of Fig. 4, because a larger Ω_m (i.e., more matter and less DE) will correspond to a weaker effect of anti-gravity. This shows that adopting different FA recipe will also affect the expanding history of the universe.

4. CONCLUSION AND DISCUSSION

The control of the systematic uncertainties of SNe Ia has become a fundamental topic of precision cosmology. Flux-averaging, which is proposed in (Wang 2000), has been

proved to be a very useful technique to reduce the systematic uncertainties of SNe Ia. Note that the original FA technique will lead to a significant decrease of SN data points, and thus will yield larger error bars for various model parameter. To solve this problem, an improved version of FA was proposed, in which only the SN data at high-redshift are flux-averaged (Wang & Wang 2013a). This new method relates to two quantities: z_{cut} and Δz . In previous studies, both z_{cut} and Δz are set as a specific value. For example, in (Wang & Dai 2015), Wang and Dai only considered the case of ($z_{cut} = 0.5, \Delta z = 0.04$). However, as shown in the current work, different choice of ($z_{cut}, \Delta z$) will significantly change the results of FoM , and arbitrarily choosing a FA recipe can not give the tightest DE constraints.

In this work, we have presented a systematic and comprehensive investigation on the cosmological consequences of the JLA SN sample by using the improved FA technique. Quite different from the previous studies, we have scanned the whole ($z_{cut}, \Delta z$) plane to search the best FA recipe; for each choice of ($z_{cut}, \Delta z$), we have performed a MCMC analysis for the CPL parameterization, and have calculated the corresponding value of FoM . To ensure that our results do not depend on a specific DE parameterization, we have also considered the cases of the JBP, the BA and the WANG model. Then, based on the best FA recipe obtained, we have discussed the impacts of varying z_{cut} and varying Δz . Next, combining FA with RT technique, we have revisited the evolution of β . Finally, using the JLA data alone, we have studied the impacts of adopting different FA recipe on parameter estimation.

Our conclusions are as follows:

- (1) The best FA recipe is ($z_{cut} = 0.6, \Delta z = 0.06$), which gives a largest $FoM = 4.6965$ (see Fig. 1). This result holds true for all the four DE parameterizations, and thus is insensitive to a specific DE model (see table 1).
- (2) Flux-averaging JLA samples at $z_{cut} \geq 0.4$ will yield tighter DE constraints than the case without using FA; in contrast, the effects of varying Δz are much smaller (see Fig. 2).
- (3) Using FA can significantly reduce the redshift-evolution of β for the JLA SN sample (see Fig. 3); this implies that adopting FA technique can reduce the systematic uncertainties caused by β evolution.
- (4) Adopting the best FA recipe will yield a larger fractional matter density Ω_m (see Fig. 4) and a universe with a smaller acceleration (see Fig. 5).

In summary, we present an alternative method of dealing with JLA data, which can reduce the systematic uncertainties of SNe Ia and give the tighter DE constraints at the same time. Our method will be useful in the use of SNe Ia data for precision cosmology.

There are a lot of related problems deserve further studies. For examples, the best FA recipe obtained in this work can be used to constrain various DE models (Steinhardt, Wang & Zlatev 1999; Caldwell 2002; Li 2004; Wei et al. 2005; Wang et al. 2008; Gao, Chen & Shen 2009; Li et al. 2009a; Zhang et al. 2012; Wang et al. 2016b). Besides, it can be used to explore the dynamical evolution of DE EoS by using various model-independent methods (Huterer, & Starkman 2003; Huterer, & Cooray 2005; Huang et al. 2009; Wang et al. 2011; Li et al. 2011b; Gong et al. 2013; Wang et al. 2016a; Mukherjee 2016). In addition, based on the improved FA technique,

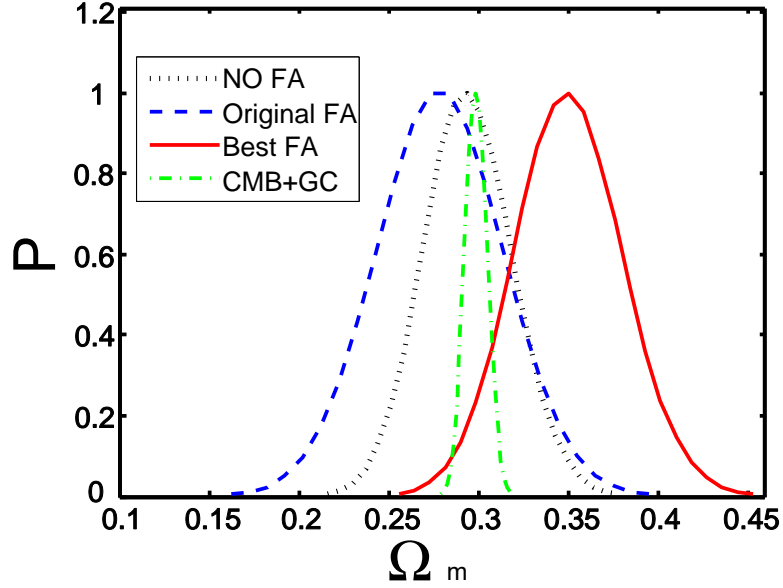


FIG. 4.— The 1D marginalized probability distributions of Ω_m given by different FA recipe, for the Λ CDM model. “No FA” (black dotted line) denotes the case without using FA, “Original FA” (blue dashed line) represents the FA recipe ($z_{cut} = 0, \Delta z = 0.06$), “Best FA” (red solid line) corresponds to the FA recipe ($z_{cut} = 0.6, \Delta z = 0.06$). The corresponding result given by the CMB+GC data (green dashed-dotted line) is also shown for comparison. Only the JLA data are used in the analysis.

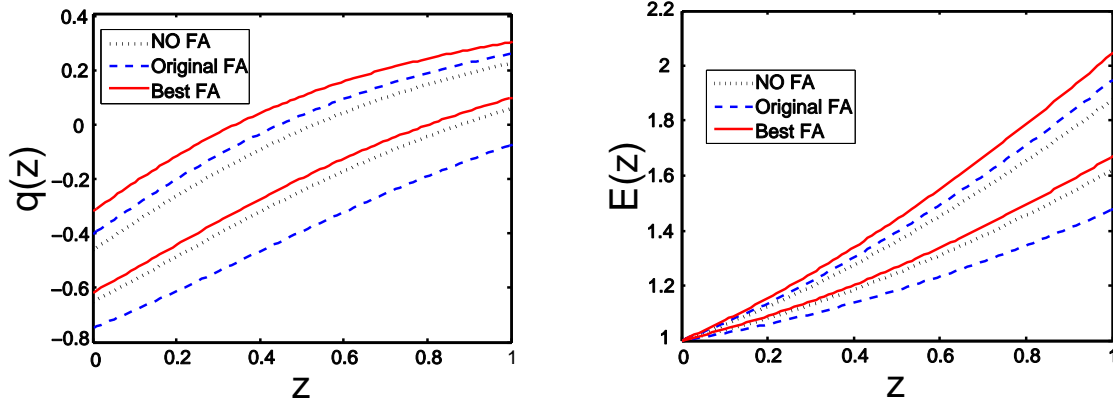


FIG. 5.— 1σ regions of $E(z)$ (left panel) and $q(z)$ (right panel) at redshift region $[0, 1]$ given by different FA recipe, for the Λ CDM model. “No FA” (the region inside black dotted lines) denotes the case without using FA, “Original FA” (the region inside blue dashed lines) represents the FA recipe ($z_{cut} = 0, \Delta z = 0.06$), “Best FA” (the region inside red solid lines) corresponds to the FA recipe ($z_{cut} = 0.6, \Delta z = 0.06$). Only the JLA data are used in the analysis.

a series of related topics, such as dark sector interaction (Li et al. 2009b), massive neutrino (Li et al. 2013b), cosmic age (Wang & Zhang 2008; Lan et al. 2010; Wang et al. 2010), cosmic fate (Li et al. 2012) and so on, need to be revisited.

In a recent work, Ma, Corasaniti and Bassett proposed a new Bayesian inference method to explore the JLA data, by applying Bayesian graphs (Ma, Corasaniti & Bassett 2016). Making use of this new analysis technique, they showed that the error bars of various model parameters can be significantly reduced. It will be very interesting to explore the current SNe

Ia data by combining this Bayesian inference method with our best FA recipe. This will be done in a future work.

SW is supported by the National Natural Science Foundation of China under Grant No. 11405024 and the Fundamental Research Funds for the Central Universities under Grant No. 16lgpy50. ML is supported by the National Natural Science Foundation of China (Grant No. 11275247, and Grant No. 11335012) and a 985 grant at Sun Yat-Sen University.

REFERENCES

- Ade, P. A. R., Aghanim, N., Arnaud, M., et al. 2015, arXiv:1502.01590
 Albrecht, A., Bernstein, G., Cahn, R. et al., arXiv:astro-ph/0609591
 Amanullah, R., et al., 2010, ApJ, 716, 712
 Anderson, L., et al., 2014, MNRAS, 441, 24
 Astier, P., et al., 2006, A&A, 447, 31
 Barboza, Jr., E. M. & Alcaniz, J. S. 2008, Phys. Rev. B, 666, 415
 Betoule, M., Kessler, R., Guy, J., et al. 2014, A&A, 568, A22
 Bengochea, G. R., & De Rossi, M. E., 2014, Phys. Lett. B, 733, 258
 Caldwell, R. R., 2002, Phys. Lett. B, 545, 23
 Chevallier, M., & Polarski, D. 2001, Int. J. Mod. Phys. D, 10, 213
 Chuang, C.-H., & Wang, Y., 2012, MNRAS, 426, 226
 Clarkson, C.; Cortes, M.; Bassett, B. A. 2007, J. Cosmology Astropart. Phys., 08, 011
 Conley, A., Guy, J., Sullivan, M., et al. 2011, ApJS, 192, 1
 Frieman J. A., Turner S. M., Huterer D., 2008, Ann. Rev. Astron. Astrophys. 46, 385
 Gao C.-J., Chen X.-L., Shen Y.-G., 2009, Phys. Rev. D, 79, 043511
 Gong, Y., Gao, Q. & Zhu Z.-H. 2013, MNRAS, 430, 3142

- Guy, J. et al., 2007, *Astron. Astrophys.* 466, 11
- Hicken M., Wood-Vasey W. M., Blondin S., et al., 2009, *ApJ*, 700, 1097
- Hicken M. et al., 2009, *ApJ*, 700, 331
- Hillebrandt W., et al., 2000, *Ann. Rev. Astron. Astrophys.* 38, 191
- Huang Q.-G., Li M., Li X.-D., Wang S., 2009, *Phys. Rev. D*, 80, 083515
- Huang Q.-G., Wang S., Wang K., 2015, *J. Cosmology Astropart. Phys.*, 12, 022
- Huterer, D. & Cooray, A. 2005, *Phys. Rev. D*, 71, 023506
- Huterer, D. & Starkman, G. 2003, *Phys. Rev. Lett.*, 90, 031301
- Jassal, H. K., Bagla, J. S., & Padmanabhan, T. 2005a, *MNRAS*, 356, L11
- Jassal, H. K., Bagla, J. S., & Padmanabhan, T. 2005b, *Phys. Rev. D*, 72, 103503
- Jha, S. et al., 2007, *ApJ*, 659, 122
- Johansson J. et al., 2013, *MNRAS*, 435, 1680
- Kessler R., et al., 2009, *ApJS*, 185, 32
- Kowalski M., et al., 2008, *ApJ*, 686, 749
- Lan, M.-X., Li, M., Li, X.-D., Wang S., 2010, *Phys. Rev. D*, 82, 023516
- Lewis, A., & Bridle, S. 2002, *Phys. Rev. D*, 66, 103511
- Li, M., 2004 *Phys. Lett. B*, 603, 1.
- Li, M., Li, X.-D., Wang, S., & Wang, Y. 2011a, *Commun. Theor. Phys.*, 56, 525
- Li, M., Li, X.-D., Wang, S., & Wang, Y. 2013a, *Frontiers of Physics*, 8, 828
- Li M., Li X.-D., Wang S., Wang Y., Zhang X., 2009b, *J. Cosmology Astropart. Phys.*, 12 014
- Li M., Li X.-D., Wang S., Zhang X., 2009a, *J. Cosmology Astropart. Phys.*, 06, 036
- Li, M., Li, N., Wang, S., Zhou, L. 2016, arXiv:1601.01451, accepted for publication in *MNRAS*
- Li, X.-D., Li, S., Wang, S., et al., 2011b, *J. Cosmology Astropart. Phys.*, 07, 011
- Li, X.-D., Wang, S., Huang, Q.-G., et al., 2012, *Sci. China Phys. Mech. Astron.*, 55, 1330
- Li, Y.-H., Wang, S., Li, X.-D., & Zhang, X. 2013b, *J. Cosmology Astropart. Phys.*, 02, 033
- Linder, E. V. 2003, *Phys. Rev. Lett.*, 90, 091301
- Ma, C., Corasaniti, P.-S., Bassett, B. A., arXiv:1603.08519
- Marriner, J. et al., 2011, *ApJ*, 740, 72
- Mohlabeng, G. M., & Ralston, J. P. 2013, *MNRAS*, 439, L16
- Mukherjee, A., 2016, *MNRAS*, 460, 273
- Perlmutter S. et al., 1999, *ApJ*, 517, 565
- Pigozzo, C.; Dantas, M. A.; Carneiro, S.; Alcaniz, J. S. 2011, *J. Cosmology Astropart. Phys.* 08, 022
- Riess A. G. et al., 1998, *AJ*, 116, 1009
- Schlaflly E. F., Finkbeiner D. P., 2011, *ApJ*, 737, 103
- Scolnic, D., Rest, A., Riess, A., et al. 2014, *ApJ*, 795, 45
- Shariff H., Jiao X., Trotta R., van Dyk D. A., arXiv:1510.05954, accepted for publication in *ApJ*
- Steinhardt P. J., Wang L. M., Zlatev I., 1999, *Phys. Rev. Lett.*, 82, 896.
- Suzuki N. et al., 2012, *ApJ*, 746, 85
- Wang, S., Geng, J. J., Hu, Y. L., & Zhang X. 2015, *Sci. China Phys. Mech. Astron.*, 58, 1
- Wang, S., Hu, Y., & Li, M., Li, N., arXiv:1501.06962, accepted for publication in *Astronomy and Astrophysics*
- Wang, S., Hu, Y., & Li, M., Li, N., 2016a, *ApJ*, 821, 60
- Wang, S., Li, N., Zhou, L., Li M., 2016b, arXiv:1605.04356
- Wang, S., Li, X.-D. & Li, M. 2010, *Phys. Rev. D*, 82, 103006
- Wang, S., Li, X.-D. & Li, M. 2011, *Phys. Rev. D*, 83, 023010
- Wang, S., Li, Y.-H., & Zhang, X. 2014a, *Phys. Rev. D*, 89, 063524
- Wang, S., Wang, Y.-Z., Geng, J.-J., & Zhang X. 2014b, *Eur. Phys. J. C*, 74, 314
- Wang, S., Wang, Y.-Z., & Zhang X. 2014c, *Commun. Theor. Phys.*, 62, 927
- Wang, S., & Wang, Y. 2013a, *Phys. Rev. D*, 88, 043511
- Wang S., Zhang Y., 2008, *Phys. Lett. B*, 669, 201
- Wang S., Zhang Y., Xia T.Y., 2008, *J. Cosmology Astropart. Phys.*, 10, 037
- Wang Y., 2000, *ApJ*, 536, 531
- Wang, Y. 2008, *Phys. Rev. D*, 77, 123525
- Wang, Y. 2009, *Phys. Rev. D*, 80, 123525
- Wang, Y.; Chuang, C.-H.; & Mukherjee, P., 2012, *Phys. Rev. D*, 85, 023517
- Wang, Y. and Dai, M., arXiv:1509.02198
- Wang, Y., & Mukherjee, P. 2004, *ApJ*, 606, 654
- Wang, Y., & Mukherjee, P. 2006, *ApJ*, 650, 1
- Wang, Y., & Mukherjee, P. 2007, *Phys. Rev. D*, 76, 103533
- Wang, Y., & Tegmark, M., 2004, *Phys. Rev. Lett.* 92, 241302
- Wang, Y., & Tegmark, M., 2005, *Phys. Rev. D* 71, 103513
- Wang, Y., & Wang, S. 2013b, *Phys. Rev. D*, 88, 043522
- Wei H., Cai R.-G., Zeng D.-F., 2005, *Class. Quant. Grav.* 22, 3189
- Weinberg, D. H., Mortonson, M. J., Eisenstein, D.J., et al. 2013, *Physics Reports*, 530, 87
- Zhang, W.-S., Cheng, C., Huang, Q.-G., et al. 2012, *Sci. China Phys. Mech. Astron.*, 55, 2244